BIOCHEMISTRY
including biophysical chemistry & molecular biology

Rapid Report

pubs.acs.org/biochemistry

Depurination of N7-Methylguanine by DNA Glycosylase AlkD Is Dependent on the DNA Backbone

Emily H. Rubinson,[†,§] Plamen P. Christov,[‡] and Brandt F. Eichman*[,†]

[†]Department of Biological Sciences, Vanderbilt University, Nashville, Tennessee 37232, United States

[‡]Vanderbilt Institute of Chemical Biology Synthesis Core, Vanderbilt University School of Medicine, Nashville, Tennessee 37232, United States

Supporting Information

ABSTRACT: DNA glycosylase AlkD excises N7-methylguanine (7mG) by a unique but unknown mechanism, in which the damaged nucleotide is positioned away from the protein and the phosphate backbone is distorted. Here, we show by methylphosphonate substitution that a phosphate proximal to the lesion has a significant effect on the rate enhancement of 7mG depurination by the enzyme. Thus, instead of a conventional mechanism whereby protein side chains participate in N-glycosidic bond cleavage, AlkD remodels the DNA into an active site composed exclusively of DNA functional groups that provide the necessary chemistry to catalyze depurination.

DNA glycosylases liberate aberrant nucleobases from the genome by catalyzing the hydrolysis of the N-glycosidic bond. Most glycosylases flip the target nucleobase into an active site that contains conserved side chains necessary for general acid−base catalysis (Figure 1A).[1] Kinetic isotope effects and quantum

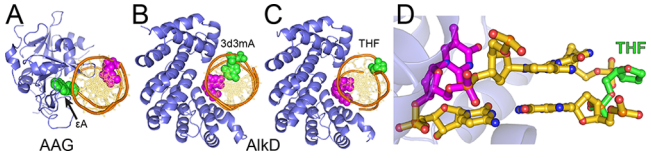

Figure 1. AlkD traps the lesion away from the protein. (A) Crystal structure of human alkyladenine DNA glycosylase (AAG) in complex with 1,N^6-ethenoadenine (εA)-DNA. (B and C) Crystal structures of AlkD in complex with (B) 3-deaza-3-methyladenine (3d3mA)-DNA and (C) tetrahydrofuran (THF)-DNA. The modified base pairs are rendered as CPK spheres, with εA, 3d3mA, and THF colored green and the opposing thymidine colored magenta. (D) Side view of the extrahelical THF-T bulge trapped by AlkD (blue).

mechanical calculations for several monofunctional DNA and RNA glycosylases are consistent with a dissociative (D_N*A_N) mechanism involving a cationic oxocarbenium intermediate that is converted to an abasic site by a water nucleophile.[2−7] Catalysis by a variety of glycosylases is driven largely by a conserved carboxylate side chain, which can electrostatically stabilize the oxocarbenium intermediate and/or activate the water nucleophile.[8−11] In the case of purine excision, a general acid protonates N7 to activate the nucleobase leaving group.[4−7,12−15] In addition to protein functional groups, the DNA backbone has been shown to play a role in base excision by several enzymes.[4,7,16−18] The best studied example is human uracil DNA glycosylase, in which DNA phosphates promote glycosidic bond cleavage by stabilizing the charge or conformation of the oxocarbenium intermediate.[4,7,16,17,19−21]

N3- and N7-alkylated purine nucleobases are highly detrimental to the cell.[22,23] 3mA and a ring-opened formamidopyrimidyl derivative of 7mG, 2,6-diamino-4-hydroxy-N^5-methylformamidopyrimidine, are cytotoxic by virtue of their ability to inhibit DNA synthesis.[24−26] As a consequence of their positively charged purine rings, 3mA and 7mG are highly susceptible to spontaneous depurination, leading to formation of abasic sites that are both cytotoxic and mutagenic.[27−29] Thus, glycosylase excision of cationic 3mA and 7mG does not require activation by a general acid or a substantial amount of catalytic power.[6] Interestingly, most 3mA-specific glycosylases retain excision activity in the absence of specific catalytic residues, suggesting that direct side chain chemistry does not fully account for the observed rate enhancements by these enzymes.[30−34] Because spontaneous depurination rates of N7-alkylguanines depend on the DNA secondary structural context,[14,35−37] it is reasonable to postulate that the specific DNA conformation in the vicinity of the lesion contributes to excision of these adducts, although this idea has not been explored in any detail.

We recently determined several crystal structures of a unique 3mA/7mG DNA glycosylase, AlkD, in complex with alkylpurine, mismatched, and abasic DNA, all of which exhibit the same general protein−DNA binding regime.[34,37−40] AlkD does not flip the lesion into a binding pocket but instead binds the undamaged DNA strand and positions the lesion on the opposite face of the DNA helix from the protein binding surface (Figure 1B,C). Most strikingly, there are no contacts between the protein and the lesion. The alkylpurine and mismatched base pairs are highly sheared but remain stacked in the duplex, whereas the abasic site and its opposite nucleotide are rotated out of the helix to create a one-nucleotide bubble with the flanking base pairs stacked (Figure 1D). This distortion to the DNA backbone positions the flipped ribose ring closer to the phosphate of the nucleotide immediately 5′ to the lesion [position M1 (Figure 2)]. The distance between this M1 phosphate and C1′ of the flipped nucleotide is 20% shorter than in the unflipped AlkD alkylpurine/mismatch complexes and in normal B-DNA (Figure S3 of the Supporting Information).

Received: August 29, 2013
Revised: September 30, 2013
Published: October 4, 2013

   dx.doi.org/10.1021/bi401195r | *Biochemistry* 2013, 52, 7363−7365

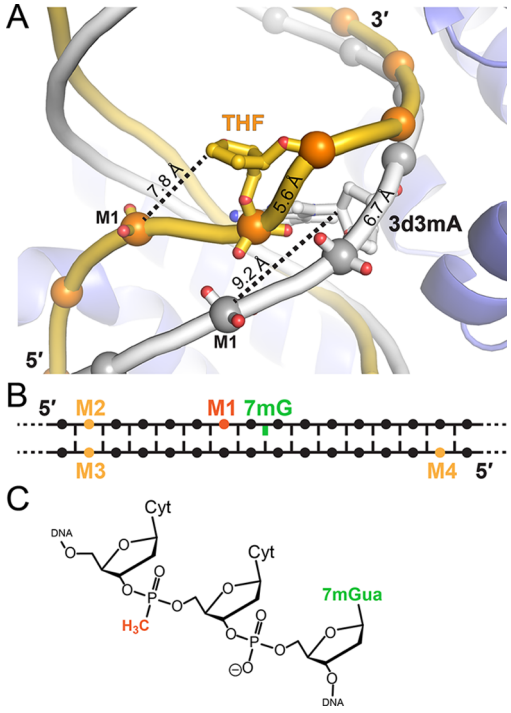

Figure 2. (A) Overlay of AlkD THF-DNA (gold) and 3d3mA-DNA (gray) complexes. The phosphate 5′ to the lesion is designated M1. Distances between M1 and C1′ of the lesion are marked with dashed lines, and distances between the phosphates covalently attached to the lesion are shown on the backbone. (B) Schematic showing the relative positions of 7mG and MeP substitutions used in this study. (C) Chemical structure of MeP in the M1 sequence context.

The skewed DNA conformation and the absence of protein contacts to the lesion in the AlkD-DNA complex led us to hypothesize that the phosphate backbone plays a substantial role in 7mG depurination. To test this, we measured the rates of AlkD-catalyzed and spontaneous release of 7mG from oligonucleotides containing nonbridging methylphosphonate (MeP) substitutions at various phosphate positions (Figure 2B). MeP eliminates the negative charge at that position (Figure 2C) and was a key strategy in determining the importance of phosphates to UDG catalysis.[16,17] We introduced a MeP at the proximal nucleotide 5′ to the 7mG (M1), and as controls for general effects of MeP substitution, at three sites located six nucleotides from the lesion and outside of the protein binding region on both damaged (M2) and undamaged (M3 and M4) strands (Figure 2B).

Compared to the substrate containing no MeP (M0), control sequences M2 and M3 had no effect on either the AlkD single-turnover (k_{st}) or nonenzymatic (k_{non}) rates of 7mG depurination, and M4 had an only modest (3-fold) effect on k_{st} (Table 1 and Figure S4 of the Supporting Information). In contrast, the M1 substitution resulted in a 15-fold reduction in AlkD activity and a 30-fold (96%) reduction in rate enhancement (k_{st}/k_{non}) compared to those of M0 (Table 1). Thus, excision of 7mG by AlkD is largely dependent on the conformation of the phosphate backbone in the vicinity of the lesion. Interestingly, the modest increase in k_{non} for M1-MeP is similar to that of 7mG depurination from single-stranded DNA (2.8×10^{-6} s^{-1}),[37] suggesting that the MeP substitution perturbs the secondary structure of the unbound DNA. Regardless of this effect, the larger effect of MeP substitution on the AlkD-catalyzed rate versus the spontaneous rate of 7mG depurination indicates that

Table 1. Rates of AlkD-Catalyzed and Spontaneous Depurination of 7mG from MeP-DNA

	k_{st} ($\times 10^{-3}$ s^{-1})[a]	k_{non} ($\times 10^{-6}$ s^{-1})[a]	k_{st}/k_{non}
M0	23.6 ± 1.1	1.0 ± 0.1	2.4×10^4
M1	1.6 ± 0.4	1.8 ± 0.2	8.9×10^2
M2	23.6 ± 1.1	1.0 ± 0.1	2.4×10^4
M3	23.2 ± 1.2	1.1 ± 0.03	2.1×10^4
M4	7.7 ± 0.5	1.1 ± 0.1	7.0×10^3

[a]Single-turnover (k_{st}) and nonenzymatic (k_{non}) rate constants for depurination of 7mG from 25-mer oligonucleotides at 37 °C, pH 7.5, and an ionic strength of 150 mM. M1−M4 each contained one MeP at the positions shown in Figure 2B. Data for M0 (no MeP) were taken from ref 37. DNA sequences and kinetic data can be found in the Supporting Information.

the 96% reduction in M1/M0 rate enhancement is attributed to the specific enzyme-DNA complex and not to an effect on the DNA alone.

The residual 7mG depurination activity in the M1 substrate may stem from the phosphates immediately 5′ and 3′ to the lesion, which reside 5 Å from C1′ of the lesion in the flipped THF complex (Figure S3 of the Supporting Information). However, we were unable to substitute MeP at these positions because of the manner in which the 7mG substrate was prepared (see the Supporting Information). Although these flanking phosphates are closer to the lesion than M1, only M1 moves closer to the lesion upon base flipping (Figure S3 of the Supporting Information). The modest reduction in the level of excision of 7mG from the M4 substrate is consistent with preferential binding of the enzyme to the unmodified strand and may reflect a preference of the enzyme to initially bind the 5′ ends of an oligonucleotide.

Given the absence of protein functional groups in the vicinity of the lesion, we conclude that catalysis of 7mG excision by AlkD is driven by the DNA and speculate that the proximal phosphates facilitate depurination by either stabilizing the oxocarbenium intermediate or positioning the attacking water. Introduction of MeP, which eliminates the negative charge and replaces a polar oxygen with an aliphatic methyl group, could have effected either the electrostatic environment or the specific conformation of the DNA. The decrease in the distance from the M1 phosphate to the lesion upon base flipping suggests that the observed effect of MeP substitution may have disrupted a stabilizing electrostatic interaction between the anionic phosphate backbone and the oxocarbenium (Figure 3). For this to be true, however, the M1 phosphate would need to be closer to the lesion than in the THF structure (observed distance of 7.8 Å), and it is not unreasonable to postulate that a cationic 3mA or 7mG substrate would have such an additional distortive effect. Alternatively, the phosphate group may stabilize a particular DNA conformation necessary for catalysis. Indeed, the nucleic acid secondary structure is the basis for designed DNAs (DNAzymes) that catalyze various metal-dependent RNA cleavage and DNA ligation reactions.[41,42] In addition to a direct interaction, the phosphate could deprotonate or stabilize any developing positive charge on the attacking water. Regardless of the specific mechanism employed, this work, together with the crystal structures, establishes that the specific conformation of the DNA backbone captured by the enzyme positions the phosphate for catalysis. To the best of our knowledge, this is the first example of an active site composed exclusively of DNA atoms.

dx.doi.org/10.1021/bi401195r | *Biochemistry* 2013, 52, 7363−7365

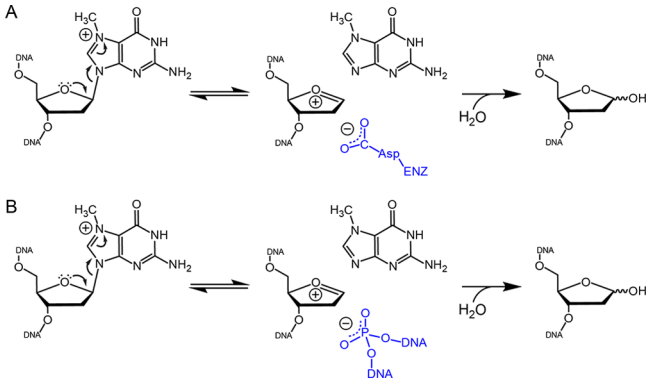

Figure 3. Protein and/or DNA functional groups provide an anionic environment to drive base excision. The chemical mechanism of 7mG depurination is shown, with stabilization of the oxocarbenium reaction intermediate by (A) a conserved carboxylate side chain and (B) a DNA phosphate moiety.

■ ASSOCIATED CONTENT

Supporting Information

Experimental procedures and representative kinetic data. This material is available free of charge via the Internet at http://pubs.acs.org.

■ AUTHOR INFORMATION

Corresponding Author

*E-mail: brandt.eichman@vanderbilt.edu. Phone: (615) 936-5233.

Present Address

§E.H.R.: Physical Science Department, Avon Products, Inc., Suffern, NY 10901.

Funding

This work was supported by a grant from the National Science Foundation (MCB-1122098). Additional support for facilities was provided by the Vanderbilt Center in Molecular Toxicology (P30 ES000267) and the Vanderbilt-Ingram Cancer Center (P30 CA068485). E.H.R. was supported by the Vanderbilt Training Program in Environmental Toxicology (National Institutes of Health Grant T32 ES07028).

Notes

The authors declare no competing financial interest.

■ REFERENCES

(1) Brooks, S. C., Adhikary, S., Rubinson, E. H., and Eichman, B. F. (2013) *Biochim. Biophys. Acta 1834*, 247−271.

(2) Werner, R. M., and Stivers, J. T. (2000) *Biochemistry 39*, 14054−14064.

(3) Chen, X. Y., Berti, P. J., and Schramm, V. L. (2000) *J. Am. Chem. Soc. 122*, 1609−1617.

(4) Dinner, A. R., Blackburn, G. M., and Karplus, M. (2001) *Nature 413*, 752−755.

(5) McCann, J. A., and Berti, P. J. (2008) *J. Am. Chem. Soc. 130*, 5789−5797.

(6) Stivers, J. T., and Jiang, Y. L. (2003) *Chem. Rev. 103*, 2729−2759.

(7) Berti, P. J., and McCann, J. A. (2006) *Chem. Rev. 106*, 506−555.

(8) Drohat, A. C., Jagadeesh, J., Ferguson, E., and Stivers, J. T. (1999) *Biochemistry 38*, 11866−11875.

(9) Labahn, J., Scharer, O. D., Long, A., Ezaz-Nikpay, K., Verdine, G. L., and Ellenberger, T. E. (1996) *Cell 86*, 321−329.

(10) Hollis, T., Ichikawa, Y., and Ellenberger, T. (2000) *EMBO J. 19*, 758−766.

(11) Norman, D. P., Chung, S. J., and Verdine, G. L. (2003) *Biochemistry 42*, 1564−1572.

(12) Brinkmeyer, M. K., Pope, M. A., and David, S. S. (2012) *Chem. Biol. 19*, 276−286.

(13) Chen, X. Y., Berti, P. J., and Schramm, V. L. (2000) *J. Am. Chem. Soc. 122*, 6527−6534.

(14) Gates, K. S., Nooner, T., and Dutta, S. (2004) *Chem. Res. Toxicol. 17*, 839−856.

(15) O'Brien, P. J., and Ellenberger, T. (2003) *Biochemistry 42*, 12418−12429.

(16) Jiang, Y. L., Ichikawa, Y., Song, F., and Stivers, J. T. (2003) *Biochemistry 42*, 1922−1929.

(17) Parker, J. B., and Stivers, J. T. (2008) *Biochemistry 47*, 8614−8622.

(18) Rogacheva, M. V., Saparbaev, M. K., Afanasov, I. M., and Kuznetsova, S. A. (2005) *Biochimie 87*, 1079−1088.

(19) Jiang, Y. L., and Stivers, J. T. (2001) *Biochemistry 40*, 7710−7719.

(20) Werner, R. M., Jiang, Y. L., Gordley, R. G., Jagadeesh, G. J., Ladner, J. E., Xiao, G., Tordova, M., Gilliland, G. L., and Stivers, J. T. (2000) *Biochemistry 39*, 12585−12594.

(21) Bianchet, M. A., Seiple, L. A., Jiang, Y. L., Ichikawa, Y., Amzel, L. M., and Stivers, J. T. (2003) *Biochemistry 42*, 12455−12460.

(22) Beranek, D. T. (1990) *Mutat. Res. 231*, 11−30.

(23) Gates, K. S. (2009) *Chem. Res. Toxicol. 22*, 1747−1760.

(24) Boiteux, S., Huisman, O., and Laval, J. (1984) *EMBO J. 3*, 2569−2573.

(25) Larson, K., Sahm, J., Shenkar, R., and Strauss, B. (1985) *Mutat. Res. 150*, 77−84.

(26) O'Connor, T. R., Boiteux, S., and Laval, J. (1988) *Nucleic Acids Res. 16*, 5879−5894.

(27) Lawrence, C. W., Borden, A., Banerjee, S. K., and LeClerc, J. E. (1990) *Nucleic Acids Res. 18*, 2153−2157.

(28) Loeb, L. A., and Preston, B. D. (1986) *Annu. Rev. Genet. 20*, 201−230.

(29) Xiao, W., and Samson, L. (1993) *Proc. Natl. Acad. Sci. U.S.A. 90*, 2117−2121.

(30) Drohat, A. C., Kwon, K., Krosky, D. J., and Stivers, J. T. (2002) *Nat. Struct. Biol. 9*, 659−664.

(31) Cao, C., Kwon, K., Jiang, Y. L., Drohat, A. C., and Stivers, J. T. (2003) *J. Biol. Chem. 278*, 48012−48020.

(32) Eichman, B. F., O'Rourke, E. J., Radicella, J. P., and Ellenberger, T. (2003) *EMBO J. 22*, 4898−4909.

(33) Metz, A. H., Hollis, T., and Eichman, B. F. (2007) *EMBO J. 26*, 2411−2420.

(34) Rubinson, E. H., Metz, A. H., O'Quin, J., and Eichman, B. F. (2008) *J. Mol. Biol. 381*, 13−23.

(35) Vodicka, P., and Hemminki, K. (1988) *Chem.-Biol. Interact. 68*, 117−126.

(36) Lindahl, T., and Nyberg, B. (1972) *Biochemistry 11*, 3610−3618.

(37) Rubinson, E. H., Gowda, A. S., Spratt, T. E., Gold, B., and Eichman, B. F. (2010) *Nature 468*, 406−411.

(38) Rubinson, E. H., and Eichman, B. F. (2012) *Curr. Opin. Struct. Biol. 22*, 101−109.

(39) Alseth, I., Rognes, T., Lindback, T., Solberg, I., Robertsen, K., Kristiansen, K. I., Mainieri, D., Lillehagen, L., Kolsto, A. B., and Bjoras, M. (2006) *Mol. Microbiol. 59*, 1602−1609.

(40) Dalhus, B., Helle, I. H., Backe, P. H., Alseth, I., Rognes, T., Bjoras, M., and Laerdahl, J. K. (2007) *Nucleic Acids Res. 35*, 2451−2459.

(41) Breaker, R. R. (1997) *Curr. Opin. Chem. Biol. 1*, 26−31.

(42) Breaker, R. R. (1997) *Nat. Biotechnol. 15*, 427−431.

Supporting Information

Depurination of *N*7-methylguanine by DNA glycosylase AlkD is dependent on the DNA backbone

Emily H. Rubinson, Plamen P. Christov, and Brandt F. Eichman

Experimental Procedures

General Materials. The nucleoside phosphoramidites and methylphosphonamidites (Ac-dC-Me Phosphonamidite and dA-Me Phosphonamidite) were purchased from Glen Research. T4 polynucleotide kinase and DNA polymerase Klenow fragment were purchased from New England Biolabs. γ-^{32}P-ATP was purchased from American Radiolabeled Chemicals. Unmodified oligonucleotides were purchased from Integrated DNA Technologies. All other chemicals were purchased from Sigma Aldrich or Fisher Scientific. MALDI-TOF mass spectra were recorded using a 3-hydroxypicolinic acid (HPA) and ammonium hydrogen citrate matrix.

Oligonucleotide Synthesis. Methylphosphonate-containing oligodeoxynucleotides (Table S1) were synthesized on a PerSeptive Biosystems model 8909 DNA synthesizer on a 1 μmol scale using Expedite reagents (Glen Research) with the standard synthetic protocol for the coupling of the unmodified bases. Coupling of the methylphosphonamidites was performed off-line for 30 min as previously described.[1] The remainder of the synthesis was performed online using standard protocols. The DMTr group of the last base was retained. The deprotection and cleavage from the solid support of the oligonucleotides was performed with acetonitrile/ethanol/ammonium hydroxide (45:45:10) for 30 minutes at room temperature followed by addition of ethylenediamine and stirring for 6 hours at room temperature. After removal of the ammonia on a centrifugal evaporator, the oligonucleotides were purified by reverse-phase HPLC using gradient 1 and desalted. The DMTr group was removed by treatment with 2% TFA solution for 30 minutes at room temperature. The solution was neutralized with 1M ammonium hydroxide, filtered (Millex-GV®, 0.22 μm), and purified by reverse-phase HPLC. The oligonucleotides were desalted (Sephadex G-25) and characterized by MALDI-TOF mass spectrometry (Table S1 and Figure S1).

HPLC Purification. HPLC analysis was carried out on a gradient instrument (Beckman Instruments: pump module 125, photodiode array detector module 168, and System Gold software). A Phenomenex Gemini-C18 column (250 mm × 4.6 mm; flow rate, 1.5 mL/min; 250 mm × 10 mm; flow rate, 5 mL/min) was used to monitor reactions and for oligonucleotide purifications. Oligonucleotides were detected by their UV absorbance at 254 nm. The mobile phase consisted of 100 mM ammonium formate buffer in acetonitrile.

Gradient 1. Initial conditions were 5% CH_3CN (v/v); a linear gradient to 50% CH_3CN (v/v) over 20 min; a linear gradient to 80% CH_3CN (v/v) over 3 min; isocratic at 80% CH_3CN (v/v) for 2 min; then a linear gradient to the initial conditions over 3 min.

Gradient 2. Initial conditions were 1% CH_3CN (v/v); a linear gradient to 5% CH_3CN (v/v) over 5 min; a linear gradient to 10% CH_3CN (v/v) over 15 min, a linear gradient to 80% CH_3CN (v/v) over 3 min; isocratic at 80% CH_3CN (v/v) for 2 min; then a linear gradient to the initial conditions over 3 min.

Gradient 3. Initial conditions were 5% CH_3CN (v/v); a linear gradient to 8% CH_3CN (v/v) over 5 min; a linear gradient to 50% CH_3CN (v/v) over 15 min, a linear gradient to 80% CH_3CN (v/v) over 3 min; isocratic at 80% CH_3CN (v/v) for 2 min; then a linear gradient to the initial conditions over 3 min.

Table S1. Oligonucleotide sequences and masses

Name	Sequence	Calc *m/z*	Meas *m/z*
M0p	GpApCpCpApCpTpApCpApCpC	n/a	n/a
M1p	GpApCpCpApCpTpApCpApC**m**C	3556.4	3558.2
M2p	GpApCpCpApC**m**TpApCpApCpC	3556.4	3555.8
M3R	GpTpTpGpTpApApGpGpApApTpCpGpGpTpGpTpA**m**GpTpGpGpTpC	7805.1	7803.2
M4R	GpTpTpGpTpApA**m**GpGpApApTpCpGpGpTpGpTpApGpTpGpGpTpC	7805.1	7800.7
M0R	GpTpTpGpTpApApGpGpApApTpCpGpGpTpGpTpApGpTpGpGpTpC	n/a	n/a

M1p (DMTr) and M2p (DMTr) were purified by reversed-phase HPLC using gradient 1 and following DMTr deprotection using gradient 2. MALDI-TOF MS (HPA) m/z calculated for (M-H), 3556.4; found 3558.2 (M1p) and 3555.8 (M2p). M3R (DMTr) and M4R (DMTr) were purified by reversed-phase HPLC using gradient 1 and following DMTr deprotection using gradient 3. MALDI-TOF MS (HPA) m/z calculated for (M-H), 7805.1; found 7803.2 (M3R) and 7800.7 (M4R).

Oligonucleotide Labeling and Annealing. Double-stranded glycosylase substrates (M0, M1, M2, M3, and M4, Figure S2) were produced by polymerase extension of primer-template pairs as previously described.[2,3] The primer oligonucleotides (M0p, M1p, and M2p) were ^{32}P-labeled at the 5′-end, annealed to a 3-fold excess of complementary strands (M0R, M3R and M4R) in the combination M0p:M0R (M0), M1p:M0R (M1), M2p:M0R (M2), M0p:M3R (M3), M0p:M4R (M4), and extended using DNA polymerase I Klenow fragment (New England Biolabs) for 15

min at 25° C in the presence of 2′-deoxy-7-methylguanosine-5′-triphosphate (d7mGTP), dCTP, dTTP, and dATP. The Klenow extension buffer was 66 mM Tris pH 7.6, 6.6 mM $MgCl_2$, 1.5 mM β-mercaptoethanol.

AlkD Purification. *Bacillus cereus* AlkD was purified as previously described.[3] Briefly, the AlkD/pBG103 expression vector was transformed into *E. coli* HMS174 cells and overexpressed for 3 h at 37°C after addition of 0.5 mM IPTG. The His_6-SUMO-AlkD fusion protein was purified using Ni-NTA (Qiagen) affinity chromatography, followed by liberation of the His_6-SUMO tag using PreScission Protease. Free AlkD was then purified by heparin-sepharose and gel filtration chromatography to >99% homogeneity. Purified AlkD was concentrated to 12.5 mg/ml and stored at -80° C in 20 mM Bis-Tris propane buffer (pH 6.5), 100 mM NaCl, and 0.1 mM EDTA.

Glycosylase Activity Assay. Base excision activity was measured as previously described[3] using 25mer oligonucleotide duplex substrates containing a centrally located 7mG•C base pair (Figure S2). The reaction was monitored by alkaline cleavage of the abasic DNA product as a function of time. 2 nM radiolabeled DNA duplex was incubated with 20 μM AlkD in 50 mM HEPES pH 7.5, 100 mM KCl, 10 mM DTT, and 2 mM EDTA in a 10 μl reaction at 37°C. The reaction was stopped at different times by adding 0.2 N NaOH, and heated at 70°C for 2 min. The 12mer product and remaining 25mer substrate DNA strands were separated by denaturing 20% polyacrylamide gel electrophoresis in 7M urea and quantitated by autoradiography using a GE Healthcare Typhoon 9400 scanner equipped with ImageQuant Version 5.1 software. Rate constants were calculated from single-exponential fits to the data and averaged from 3 independent experiments using Kaleidagraph (Synergy Software).

References

(1) Elmquist, C. E.; Stover, J. S.; Wang, Z.; Rizzo, C. J. *J. Am. Chem. Soc.* **2004**, *126*, 11189.
(2) Asaeda, A.; Ide, H.; Asagoshi, K.; Matsuyama, S.; Tano, K.; Murakami, A.; Takamori, Y.; Kubo, K. *Biochemistry* **2000**, *39*, 1959.
(3) Rubinson, E. H.; Metz, A. H.; O'Quin, J.; Eichman, B. F. *J. Mol. Biol.* **2008**, *381*, 13.

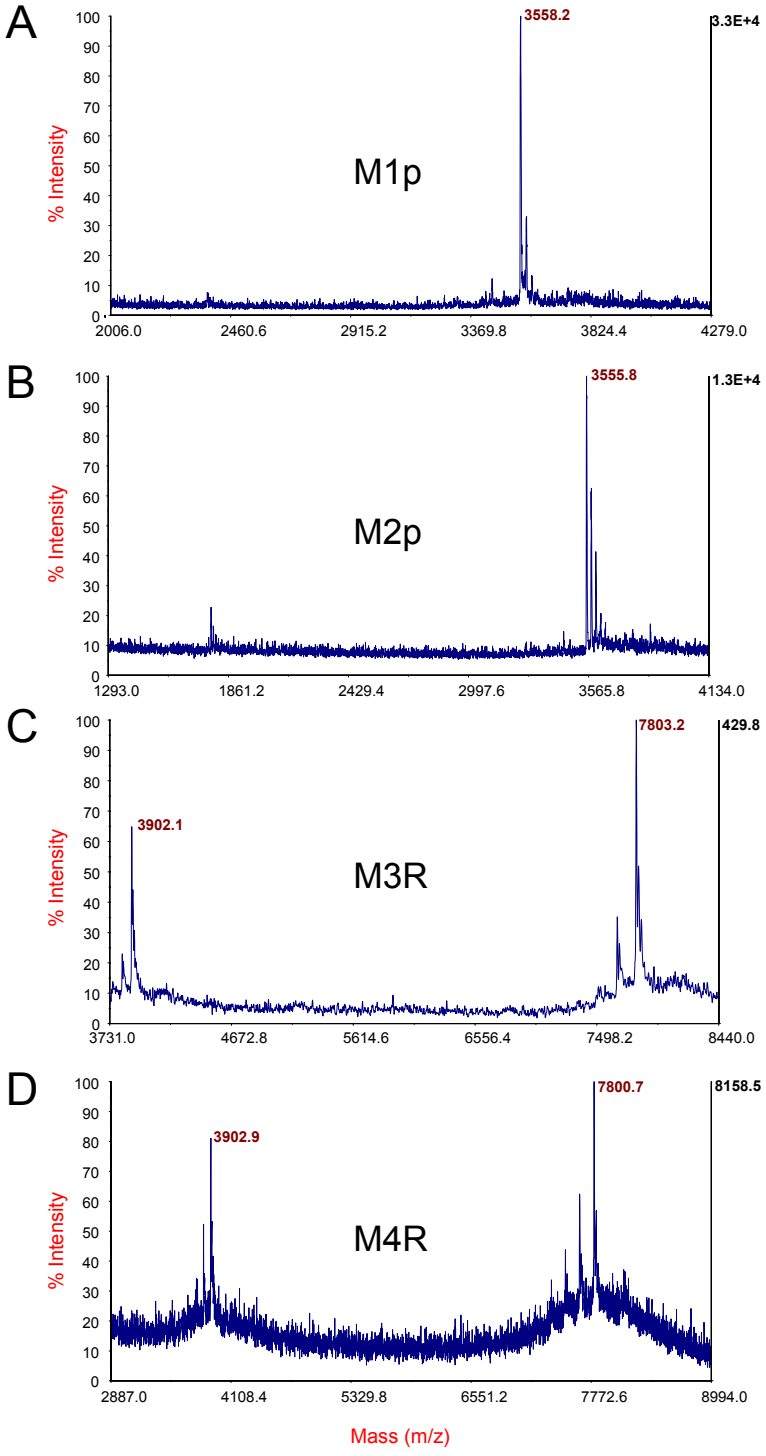

Figure S1. MALDI spectra for methylphosphonate-containing oligonucleotides. (A) M1p, (B) M2p, (C) M3R, and (D) M4R.

M0 5'-GpApCpCpApCpTpApCpApCpCpXpApTpTpCpCpTpTpApCpApApC
CpTpGpGpTpGpApTpGpTpGpGpCpTpApApGpGpApApTpGpTpTpG-5'

M1 5'-GpApCpCpApCpTpApCpApCmCpXpApTpTpCpCpTpTpApCpApApC
CpTpGpGpTpGpApTpGpTpGpGpCpTpApApGpGpApApTpGpTpTpG-5'

M2 5'-GpApCpCpApCmTpApCpApCpCpXpApTpTpCpCpTpTpApCpApApC
CpTpGpGpTpGpApTpGpTpGpGpCpTpApApGpGpApApTpGpTpTpG-5'

M3 5'-GpApCpCpApCpTpApCpApCpCpXpApTpTpCpCpTpTpApCpApApC
CpTpGpGpTpGmApTpGpTpGpGpCpTpApApGpGpApApTpGpTpTpG-5'

M4 5'-GpApCpCpApCpTpApCpApCpCpXpApTpTpCpCpTpTpApCpApApC
CpTpGpGpTpGpApTpGpTpGpGpCpTpApApGpGmApApTpGpTpTpG-5'

Figure S2. Methylphosphonate substrates for glycosylase assays. Positions of 7mG (green **X**) and methylphosphonates (red **m**) are indicated

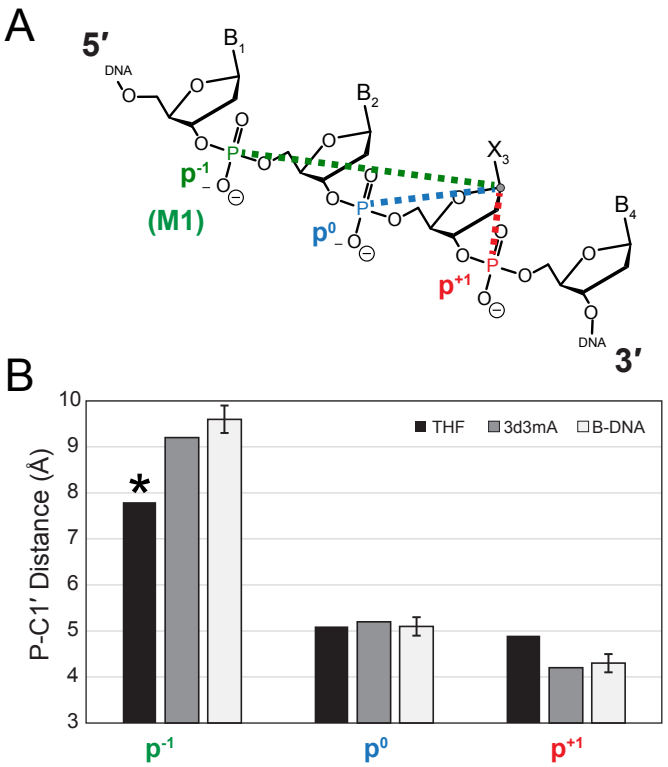

C

	THF	3d3mA	B-DNA
p^{-1}	4.9	4.2	4.3 ± 0.2
p^{0}	5.1	5.2	5.1 ± 0.2
p^{+1}	7.8	9.2	9.6 ± 0.3

Figure S3. Distortion to the DNA backbone brings THF closer to the phosphate backbone. (A) Naming convention of the phosphates (p^{-1}, p^{0}, and p^{+1}) flanking a specific base (X). Phosphate p^{-1} corresponds to position M1. (B) P-C1′ distances for flanking phosphates relative to base X in AlkD structures and free B-DNA. Values for AlkD/THF (black bars) and AlkD/3d3mA (dark grey bars) are relative to the C1′ of the THF and 3m3mA nucleotides. Values for B-DNA (light grey bars) are averaged across all nucleotides in PDB ID 1BNA. The asterisk indicates a significant decrease in distance for the THF p^{-1} phosphate. (C) Values used for the plot in panel B.

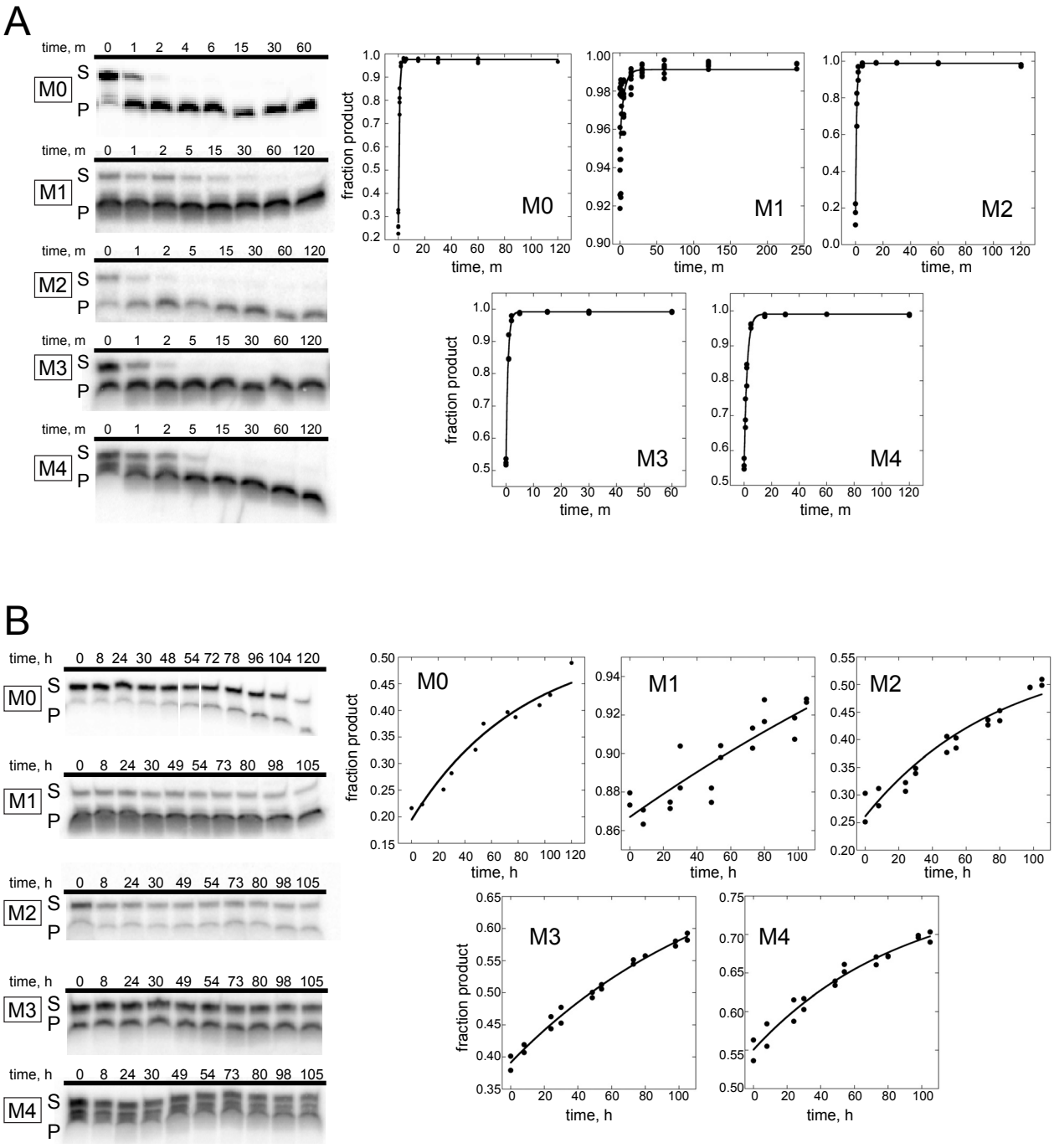

Figure S4. Raw 7mG depurination data. (A) AlkD-catalyzed and (B) spontaneous depurination of 7mG from M1-M4 DNAs. Left panels show representative denaturing polyacrylamide gels showing separation of substrate (S) and product (P) DNA as a function of time. Right panel shows quantitation of gels.